Charge- and spin-excitation gaps for a magnetic Anderson impurity embedded in a nanoscale metallic sphere

P. Schlottmann
Department of Physics, Florida State University, Tallahassee, Florida 32306
(Received 19 November 2001; published 18 April 2002)

A magnetic Anderson impurity ($S=1/2$ and $U\to\infty$) placed at the center of a nanosized metallic sphere is considered. The localized *f* electrons are hybridized with the metallic states via a contact potential, such that only *s* states interact with the impurity. In nanoscale particles the conduction states have discrete energy levels, and for equally spaced energy levels for the *s* waves, the problem is reduced to the Bethe *Ansatz* solution of the Anderson impurity model in a finite box. The Bethe *Ansatz* equations are solved numerically for the ground state and the lowest energy charge and spin excitations. The energies of the states increase monotonically with the *f*-level energy. For an even number of electrons in the system (in *s* states and localized at the impurity), the impurity in the ground state is spin compensated into a spin singlet via the Kondo effect. The specific heat and the susceptibility are exponentially activated at low *T* due to the discreteness of the energy spectrum, with the gaps given by the lowest-energy charge and spin excitations. The model also represents a quantum dot as a side branch to a short quantum wire.

DOI: 10.1103/PhysRevB.65.174407 PACS number(s): 75.20.Hr, 75.75.+a, 73.22.−f

I. INTRODUCTION

The Anderson impurity is the traditional model for the formation of a magnetic moment in a metallic solid. The extended conduction states of the metal hybridize with the highly correlated localized *f* states of the impurity. The interplay of the interactions yields a magnetic moment at intermediate temperatures, which is compensated into a singlet state via the Kondo effect at low temperatures.[1,2] Because of the spin and charge separation, there are two energy scales involved in the process: namely, the Kondo temperature T_K, which is the characteristic energy scale of the spin compensation, and the energy for the charge promotion at the impurity site. The properties of the impurity are essentially independent of the dispersion of the conduction states and of the momentum dependence of the hybridization, so that frequently a dispersion linear in the momentum and a contact hybridization are chosen. Due to the latter, only *s*-wave states are scattered and need to be retained, so that the problem effectively is a one-dimensional one.

In small metallic clusters the spacing of the energy states is determined by the finite size of the system. The discreteness of the energy spectrum has dramatic consequences on the low-temperature properties.[3,4] The physics of the Kondo effect in a finite-size metallic particle depends on the average energy spacing of the *s* states close to the Fermi level, but is not expected to be very sensitive to the details of the discrete spectrum of the occupied or empty conduction states. The Anderson impurity in an ultrasmall metallic grain has been studied previously using the noncrossing diagram approximation.[5] It was found that the Kondo resonance is strongly affected when the mean level spacing is comparable to T_K and it also depends on the parity of the number of electrons. An Anderson-impurity-like model in a finite-size system was also studied by Buttiker and Stafford[6] in the context of tunneling into a quantum dot embedded or as a side branch to a small metallic ring (see also Ref. 7).

Within the framework of the Kondo model (impurity spin represented by a spin 1/2 interacting via spin exchange with conduction states) an impurity placed at the center of a nanosized sphere and equal energy spacings for the levels in the host has been mapped onto the Kondo Hamiltonian solved by Andrei[8] and Wiegmann[9] via Bethe's *Ansatz*. This formulation was used[10] to calculate all the energy levels and the thermodynamics of a system of three and five electrons in *s* states (corresponding to 19 and 91 electrons in the sphere, respectively). The ground state and lowest-energy excitation involving no spin flip and one spin flip were also studied for larger systems. These excitations define the gaps for the leading exponential activation energies of the specific heat and the susceptibility.

In this paper we study an Anderson impurity placed at the center of a nanosized metallic sphere. The main difference with the standard mixed-valence problem is that the energy spectrum of the host is now discrete. Similarly to the Kondo impurity,[10] the problem can be mapped onto the Bethe *Ansatz* solution of the Anderson model.[2,11] The model and the Bethe *Ansatz* equations diagonalizing it are summarized in Sec. II. The low-energy states correspond to two-strings, which for a finite system may lead to spurious solutions of the Bethe *Ansatz* equations. It is therefore convenient to reformulate the model in terms of holes[12] rather than electrons (Sec. III). The Bethe *Ansatz* equations have now solutions with real (rather than complex) rapidities for low-energy states. We present the solutions for the ground state and the first charge and spin (singlet and triplet) excitations for the finite system. These excitation energies define the gaps for the leading exponential activation energies of the specific heat and the susceptibility. Conclusions follow in Sec. IV.

II. MODEL, BETHE *ANSATZ* EQUATIONS, AND SPIN-PAIRED STATES

A. Model

In a nanoscale metallic sphere with an Anderson impurity at its center and a contact hybridization, only *s* waves can

interact with the impurity. Since all s waves have the same spectral weight at the origin, the hybridization matrix element V is independent of the host state and the Hamiltonian has the usual form

$$H=\sum_{i\sigma}\ \epsilon_i c_{i\sigma}^{\dagger}c_{i\sigma}+\epsilon_f\sum_{\sigma}\ |\sigma\rangle\langle\sigma|$$

$$+V\sum_{i\sigma}\ [c_{i\sigma}^{\dagger}|0\rangle\langle\sigma|+|\sigma\rangle\langle 0|c_{j\sigma}], \tag{1}$$

where i labels the s states of energies ϵ_i, ϵ_f is the energy of the localized f level, and the bras and kets denote the three states of the impurity: 0 for the empty configuration and $\sigma=\uparrow,\downarrow$ for the singly occupied states. The doubly occupied impurity state is excluded by an infinite Coulomb repulsion. Consequently, the impurity states do not have fermionic commutation relations.

The properties of the impurity depend on the average energy spacing of the host states close to the Fermi level, but are not expected to be very sensitive to the details of the discrete spectrum of the occupied or empty conduction states. For simplicity we choose equal energy spacings for the levels, which is characteristic of particles in a one-dimensional box with periodic boundary conditions and a linear dispersion. This approximation is usually also adopted in the thermodynamic limit, where it corresponds to a constant density of states. In addition we consider only forward-moving particles to avoid the degeneracy of states with momentum k and $-k$. The model is now equivalent to the solution of the Hamiltonian

$$\mathcal{H}=\sum_{\sigma}\ \int dx\ c_{\sigma}^{\dagger}(x)\left(-i\frac{\partial}{\partial x}\right)c_{\sigma}(x)+\epsilon_f\sum_{\sigma}\ |\sigma\rangle\langle\sigma|$$

$$+V\sum_{\sigma}\ \int dx\ \delta(x)[c_{\sigma}^{\dagger}(x)|0\rangle\langle\sigma|+|\sigma\rangle\langle 0|c_{\sigma}(x)], \tag{2}$$

with periodic boundary conditions in the interval $(-L/2,L/2)$. The above model is identical to the Anderson Hamiltonian solved in Refs. 2 and 11 via Bethe's *Ansatz*.

B. Bethe *Ansatz* equations

The model (2) is diagonalized by means of two nested Bethe *Ansätze* in terms of a set of N charge rapidities $\{k_j\}$ and a set of M spin rapidities $\{\lambda_\alpha\}$. These rapidities satisfy the following Bethe *Ansatz* equations[2,11]

$$\exp(ik_jL)e_1(k_j-\epsilon_f)=\prod_{\alpha=1}^{M}\ e_1(k_j-\lambda_\alpha),$$

$$\prod_{j=1}^{N}\ e_1(\lambda_\alpha-k_j)=-\prod_{\beta=1}^{M}\ e_2(\lambda_\alpha-\lambda_\beta), \tag{3}$$

where $e_m(\lambda)=(\lambda-imV^2/2)/(\lambda+imV^2/2)$, $j=1,\ldots,N$, and $\alpha=1,\ldots M$. Rapidities within one set have to be all different (otherwise the wave function vanishes identically). The magnetization and the energy of the system are given by

$$S_z=\frac{1}{2}N-M,\quad E=\sum_{j=1}^{N}\ k_j. \tag{4}$$

In the thermodynamic limit ($L\to\infty$ keeping N/L and M/L fixed) and in the ground state, the charge rapidities form M complex conjugated pairs of imaginary part $V^2/2$ and real part equal to a spin rapidity, $k_{\pm}=\lambda\pm V^2/2$, and $N-2M$ real k. The former represent spin-paired electrons, while the latter correspond to unpaired electrons contributing to the magnetization. The ground state then consists of two sets of solutions: $\{\lambda_\alpha\}$ ($\alpha=1,\ldots,M$ for the paired electrons) and $\{k_j\}$ ($j=1,\ldots,N-2M$ for unpaired electrons). In zero field we have $N=2M$ such that all electrons are paired.

In a small system (L is finite) the charge rapidities still form two-strings in the ground state, but the imaginary part of the string differs from $V^2/2$ and the real part is not equal a spin rapidity. The deviations in the real and imaginary parts are a function of L. For sufficiently large L the deviations are exponentially small. In general, for finite L, the solutions of the Bethe *Ansatz* equations have to be obtained numerically.

C. Spin-paired states

To understand the difficulties in obtaining solutions involving spin-paired electrons we consider here the situation $N=2$ and $M=1$, i.e., two electrons, one with up spin and the other one with down spin. The ground state is characterized by a real spin rapidity λ and a pair of complex conjugated k rapidities, $k_{\pm}=\kappa\pm i\chi$, which satisfy the nonlinear equations

$$e^{i\kappa L}e^{\mp\chi L}=\frac{\kappa-\epsilon_f+i(\frac{1}{2}V^2\pm\chi)}{\kappa-\epsilon_f-i(\frac{1}{2}V^2\mp\chi)}\,\frac{\kappa-\lambda-i(\frac{1}{2}V^2\mp\chi)}{\kappa-\lambda+i(\frac{1}{2}V^2\pm\chi)},$$

$$1=\frac{\lambda-\kappa-i(\frac{1}{2}V^2+\chi)}{\lambda-\kappa+i(\frac{1}{2}V^2+\chi)}\,\frac{\lambda-\kappa-i(\frac{1}{2}V^2-\chi)}{\lambda-\kappa+i(\frac{1}{2}V^2-\chi)}. \tag{5}$$

The last equation immediately yields $\lambda=\kappa$. It is convenient to rewrite the first equation as

$$\kappa=\frac{\pi}{L}(J_\alpha-\tfrac{1}{2})-\frac{1}{L}\arctan\left[\frac{(\kappa-\epsilon_f)^2+(\chi^2-\frac{1}{4}V^4)}{(\kappa-\epsilon_f)V^2}\right],$$

$$e^{-2\chi L}=\left(\frac{\chi-\frac{1}{2}V^2}{\chi+\frac{1}{2}V^2}\right)^2\frac{(\kappa-\epsilon_f)^2+(\frac{1}{2}V^2+\chi)^2}{(\kappa-\epsilon_f)^2+(\frac{1}{2}V^2-\chi)^2}, \tag{6}$$

which determines κ and χ. Here J_α is an integer (quantum number) which arises from the periodic boundary conditions. The energy is given by $E=2\kappa$.

We first analyze the solutions of the second equation of Eqs. (6) for large $|\kappa-\epsilon_f|$. The solid line in Fig. 1(a) displays the right-hand side for $|\kappa-\epsilon_f|=100V^2$ as a function of χ/V^2. The dash-dotted line shows the left-hand side (exponential) for $L=2$. There are two solutions to the equation: namely, $\chi=0$ and $\chi=\frac{1}{2}V^2+\delta$, with δ being a positive number. The $\chi=0$ solution leads to two identical real rapidities

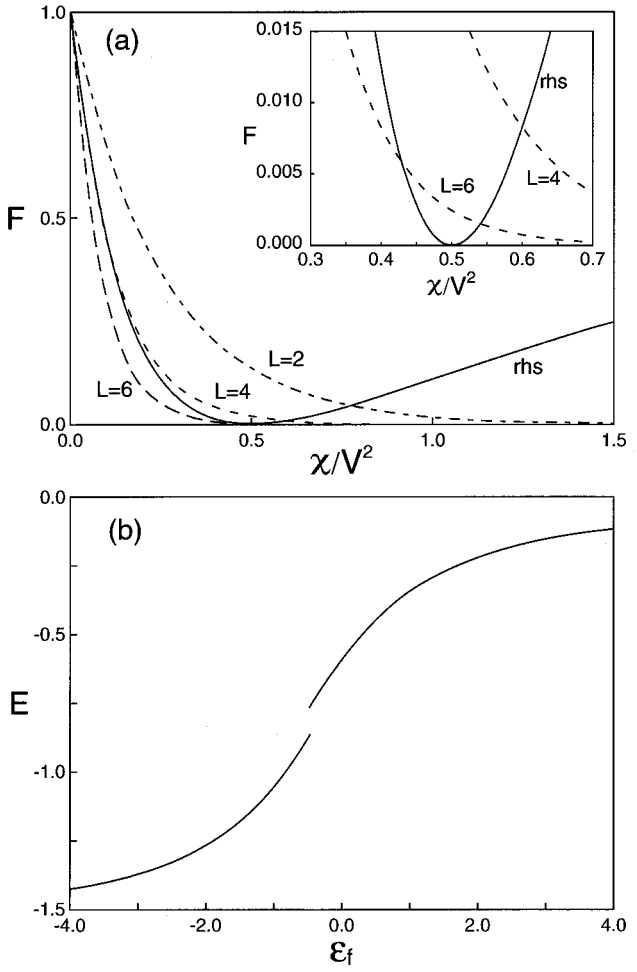

FIG. 1. (a) Solutions of the second equation of Eqs. (6) ($N=2$ and $M=1$) for $V=1$ and $|\kappa-\epsilon_f|=100V^2$. F represents the right-hand side (solid line) and the left-hand side (exponential) of the equation. The dash-dotted line corresponds to $L=2$, the dashed curve to $L=4$, and the long-dashed curve to $L=6$. Intersections refer to possible solutions. The inset shows the blown-up behavior for $\chi\approx V^2/2$. (b) Energy as a function of ϵ_f for $N=2$, $M=1$, $L=4$, $V=1$, and $J=0$. The solution (with $\chi>V^2/2$) is discontinuous when the f level is on resonance with the host state.

and hence to a vanishing wave function. Consequently, the only physical solution in this case is the second one. The dashed curve represents the exponential for $L=4$. For $L=4$ both curves are tangent to each other at $\chi=0$ (strictly if $|\kappa-\epsilon_f|=\infty$), and again we have only one physical solution with $\chi>\frac{1}{2}V^2$. The long-dashed curve corresponds to $L=6$ for which there is in addition a third solution with $\chi<\frac{1}{2}V^2$ [see also the inset to Fig. 1(a)].

Consider now the situation of small $|\kappa-\epsilon_f|$. When $\kappa\rightarrow\epsilon_f$ (resonance condition) also χ has to approach the value $V^2/2$, and from the second equation of Eqs. (6) we obtain that approximately $\chi-V^2/2\approx|\kappa-\epsilon_f|\exp(-V^2L/2)$. From the first equation of Eqs. (6) the solution for κ is discontinuous at the resonance and the energy as a function of ϵ_f has a jump proportional to $(2/L)\exp(-LV^2/2)$ (note that in the thermodynamic limit there is no discontinuity). The energy given by the numerical solution of Eqs. (6) is shown in Fig. 1(b) for $J_\alpha=0$, $V=1$, and $L=4$.

As discussed above, for sufficiently large L ($L>4$ for the parameters used in Fig. 1),[13] there is a second solution, which close to the resonance yields $\chi-V^2/2\approx-|\kappa-\epsilon_f|\exp(-V^2L/2)$. The discontinuity of the energy for this solution has the opposite sign. On the other hand, if we allow $\chi-V^2/2$ to change sign across the resonance, we obtain a solution with continuous energy. There are then four possible solutions (two continuous and two discontinuous) at the resonance. In the case of M pairs of electrons this yields 2×2^M possibilities. It is difficult to judge on physical grounds which of these is the true ground state.

A safe approach is to reformulate the problem in terms of holes rather than electrons. In terms of holes the model remains integrable and the low-energy states correspond to real rapidities within the Bethe *Ansatz* approach.

III. ALTERNATIVE FORMULATION

A. Model and Bethe *Ansatz* equations

In terms of holes the impurity states correspond to configurations with one and two particles. The latter has zero spin and is denoted with $|0\rangle$. The empty configuration is now excluded by the infinite Coulomb interaction. The creation and annihilation operators still refer to electrons. The Hamiltonian is given by[12]

$$\mathcal{H}=\sum_\sigma\int dx\, c_\sigma^\dagger(x)\left(-i\frac{\partial}{\partial x}\right)c_\sigma(x)-\epsilon_f\sum_\sigma|\sigma\rangle\langle\sigma|$$
$$+\frac{V}{\sqrt{2}}\sum_\sigma\int dx\,\delta(x)[c_\sigma^\dagger(x)|\sigma\rangle\langle0|+|0\rangle\langle\sigma|c_\sigma(x)], \tag{7}$$

where the $\sqrt{2}$ renormalizing the hybridization arises from a Clebsch-Gordan coefficient. Note that the sign of ϵ_f is reversed and the form of the hybridization has changed. The energy and the magnetization are now given by $E=\Sigma_{j=1}^N k_j$ and $S_z=\frac{1}{2}(N+1)-M$.

The Bethe *Ansatz* equations diagonalizing model (7) are[12]

$$\exp(-ik_jL)=\prod_{\alpha=1}^M e_{1/2}(k_j-\lambda_\alpha),$$
$$e_{1/2}(\lambda_\alpha-\epsilon_f)\prod_{j=1}^N e_{1/2}(\lambda_\alpha-k_j)=-\prod_{\beta=1}^M e_1(\lambda_\alpha-\lambda_\beta), \tag{8}$$

where the direction of the momentum [in $\exp(-k_jL)$] is reversed with respect to the formulation in Sec. II and the scattering phase shifts involve $e_{1/2}$ and e_1 as a consequence of the $\sqrt{2}$ renormalizion in the hybridization. The impurity phase shift now appears in the second set of Bethe *Ansatz* equations determining the spin rapidities, while in the formulation of Sec. II it affected directly the charge rapidities (first set of Bethe *Ansatz* equations).

The advantage of this formulation is that the charge rapidities do not form strings, but are all real. Hence, the

ground state and the low-energy excitations involve only real charge and spin rapidities. The numerical solution of the equations for finite L is now straightforward, in contrast to the formulation presented in Sec. II, which involves complex rapidities. In the continuum limit the ambiguities discussed in Sec. II disappear and the integral equations for the rapidity densities are equivalent.

B. Quantum numbers

Previous investigations for small size systems of other models via the Bethe *Ansatz* are the following: (1) A thorough study of short Heisenberg chains by comparing exact diagonalizations with the Bethe *Ansatz* was performed by Karbach and Müller,[14] and (2) all the energy levels and the thermodynamics for the exchange Kondo model in a small box with three and five electrons were obtained in Ref. 10. The present study [within the formulation of Eqs. (8)] is closely related to these approaches.

We now take the logarithm in both sets of equations (8) and obtain

$$\begin{aligned} Lk_j &= 2\pi I_j - \sum_{\alpha=1}^{M} \{2\arctan[4(k_j-\lambda_\alpha)/V^2]+\pi\}, \\ &\arctan[4(\lambda_\alpha-\epsilon_f)/V^2]+\sum_{j=1}^{N}\arctan[4(\lambda_\alpha-k_j)/V^2] \\ &= \pi J_\alpha + \sum_{\beta=1}^{M}\arctan[2(\lambda_\alpha-\lambda_\beta)/V^2], \end{aligned} \tag{9}$$

where $j=1,\ldots,N$, $\alpha=1,\ldots,M$, and $\{I_j\}$ and $\{J_\alpha\}$ are two sets of quantum numbers which determine the state. Here we assumed that all λ_α are real, although higher-energy excitations involve strings of spin rapiditites. The energy of the system is given by

$$\begin{aligned} E = L^{-1}&\left\{2\pi\sum_{j=1}^{N} I_j + 2\pi\sum_{\alpha=1}^{M} J_\alpha - NM\pi\right\} \\ &- \frac{2}{L}\sum_{\alpha=1}^{M}\arctan[4(\lambda_\alpha-\epsilon_f)/V^2]. \end{aligned} \tag{10}$$

The first three terms are the charge and spin contributions from the host, while the last sum arises from the impurity.

The linear dispersion of the conduction states does not provide a natural lower bound for the energy. This fact is manifested in the Bethe *Ansatz* solution through the integer quantum number I_j, which can take arbitrary values. A lower bound cutoff for the energy (or I_j) has then to be introduced *a posteriori*. Solutions involving the same set $\{J_\alpha\}$ but two sets $\{I_j\}$ with all the I_j between the two set differing by the same integer are equivalent and can be mapped onto each other by an adequate shift in all the rapidities and ϵ_f.

C. Ground state

Consider first the set $\{J_\alpha\}$. The values of J_α have to satisfy $|J_\alpha|\leqslant(N-M+2)/2$. There are $(N+1)$ electrons (N in conduction states plus one localized electron), so that a singlet ground state requires N to be odd and $M=(N+1)/2$. Hence, for the ground state, $|J_\alpha|\leqslant(M+1)/2$, with the J_α being integers if M is odd and half-integers if M is even. The value $J_\alpha=(M+1)/2$ has to be excluded because in the limit $\epsilon_f\rightarrow\infty$ it does not yield a solution on the same branch of the arctan function. On the other hand, the $\epsilon_f\rightarrow-\infty$ is physically not relevant because it corresponds to the f level below the lower band edge in the original model, Eq. (1), such that the value $J_\alpha=-(M+1)/2$ is allowed.

There are then $(M+1)$ possible values for M quantum numbers, such that one hole is to be left in the sequence $\{J_\alpha\}$. From Eq. (10) we see that the ground state corresponds to leaving the largest J_α empty; i.e., $(M-1)/2$ is the unoccupied state. For the ground state the set of $\{I_j\}$ corresponds to N consecutive integers. The origin of this sequence is not relevant, since different choices can be mapped onto each other by shifting all rapidities and ϵ_f by a given amount.

The ground-state energy for $V=\sqrt{2}$, $L=8$, $N=9$, and $M=5$ is shown in Fig. 2 as a function of ϵ_f by the solid curve. The sequence of quantum numbers is $I_j=-4,\ldots,4$ and $J_\alpha=-3,\ldots,1$.

The expectation value for the number operator of localized electrons, n_f, is given by the derivative of the energy with respect to ϵ_f (note that here we consider electrons and not holes). This quantity is bound to have values in the interval $0\leqslant n_f\leqslant 1$; as a function of ϵ_f it is maximum in the band of conduction states and decreases monotonically for large ϵ_f. The numerical solution shows a decrease in n_f below $\epsilon_f\approx-4$. The range of validity of our solution is therefore limited to $\epsilon_f\geqslant-4$ for the present choice of quantum numbers.

D. Charge excitations

Charge excitations are generated by introducing holes into the sequence of $\{I_j\}$. The charge excitation with lowest energy is obtained by changing the largest I_j value from 4 to 5, i.e., by introducing a hole in the above sequence at $I_j=4$. The energy of this state as a function of ϵ_f is displayed in Fig. 2(a) as the dash-dotted curve labeled EC1.

Similarly, we can create a hole at $I_j=3$, so that the sequence $\{I_j\}$ is $-4,\ldots,2,4,5$. The energy of this state is shown in Fig. 2(a) as the dotted curve labeled EC2. If two holes are introduced, e.g., $I_j=-4,\ldots,3,6$ (the holes correspond to 4 and 5), we obtain the dashed curve EC3 in Fig. 2(a). Note that the excitation energies for the charges are approximately given by integer multiples of $2\pi/L$.

E. Spin excitations

Two classes of elementary spin excitations have to be considered: (1) those involving no spin-flip, i.e., spin singlet excitations, and (2) excitation changing the total spin projection (spin-flip excitations).

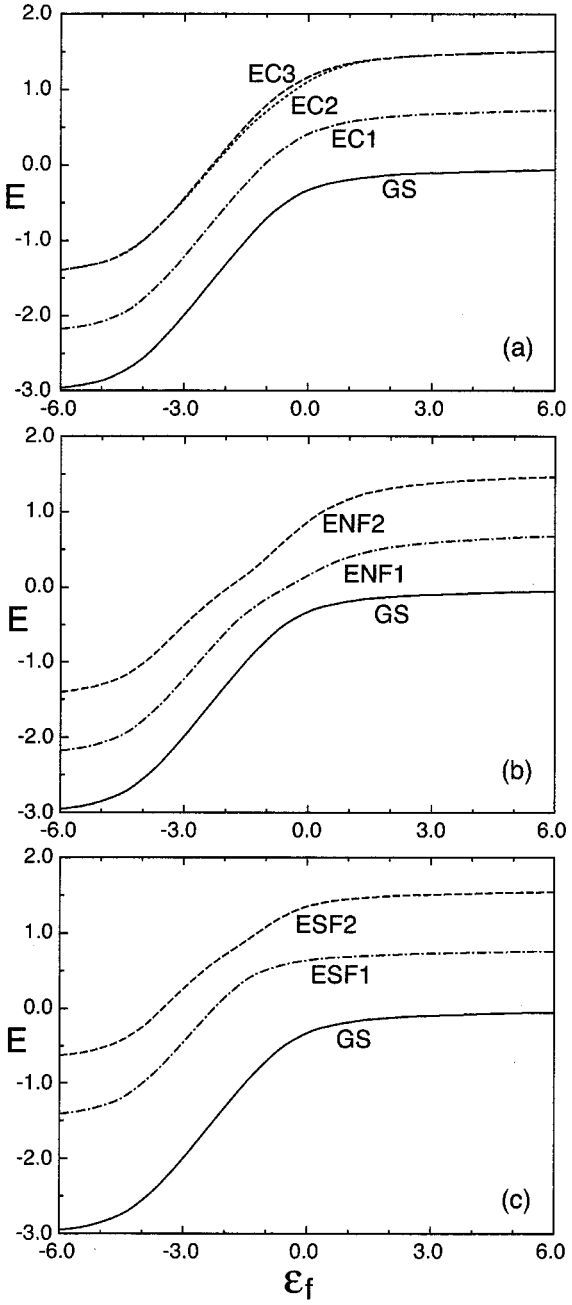

FIG. 2. Low-energy states for $V=\sqrt{2}$, $L=8$, and $N=9$ as a function of ϵ_f. The ground state is denoted by GS and shown as a thick solid line. The quantum numbers for the ground state are $I_j=-4,\ldots,4$ for the charges and $J_\alpha=-3,\ldots,1$ for the spin rapidities. (a) The charge excitations are obtained by introducing holes in the set $\{I_j\}$ as discussed in the text. (b) Spin-non-flip excitations are constructed by moving the hole in the set $\{J_\alpha\}$ as explained in the text. (c) Spin-flip excitations are obtained by reducing M to 4 and introducing holes into the sequence $\{J_\alpha\}$ (see text).

Spin excitations without spin flip are obtained by rearranging the position of the hole in the sequence $\{J_\alpha\}$. In the ground state $J_\alpha=(M-1)/2$ was unoccupied and excited states are generated if this hole is shifted to lower J_α values. For the example with $N=9$ and $M=5$ considered here, the excitation with lowest energy corresponds to the sequence $-3,\ldots,0,2$ [the hole is at $J_\alpha=1$; see dash-dotted curve labeled ENF1 in Fig. 2(b)] and the excitation with next lowest energy to $-3,-2,-1,1,2$ [the hole is at $J_\alpha=0$; see dashed line labeled ENF2 in Fig. 2(b)]. Note that here the charge quantum numbers are the same ones as in the ground state. The energy spacing between the non-spin-flip levels is approximately $2\pi/L$.

Spin-singlet excitations (without spin flip) can also be generated by introducing pairs of complex spin rapidities. In the thermodynamic limit these states reduce to so-called string states. The lowest-energy states of this class correspond to one pair of complex-conjugated λ and all other λ being real. As in Sec. II the real and imaginary parts have to be determined self-consistently in the finite box. The situation is very similar to that of a Kondo impurity in a small system.[10] The calculation is very tedious and the energy of these states is larger than that of ESF1, but comparable to ESF2.

On the other hand, spin-singlet excitations with only real rapidities do not play any role in the thermodynamic limit (there is only a finite number of them) and physics is entirely governed by the continuum of the string states of different lengths.

Spin-flip excitations are obtained by reducing M, i.e., the number of flipped spins. The lowest-energy states are obtained by flipping one spin with respect to the ground state. In our example this refers to states with $M=4$. The J_α are now half-integers and confined to the values $-7/2,\ldots,5/2$, i.e., to seven values. The state of lowest energy corresponds to the four lowest quantum numbers, i.e., $-7/2,\ldots,-1/2$. The energy of this excited state is denoted with ESF1 and shown with a dash-dotted line in Fig. 2(c). For the excited state with next lowest energy we replace $J_\alpha=-1/2$ by $1/2$, i.e., leaving a hole at $-1/2$. The state is denoted with ESF2 and plotted in Fig. 2(c) with a dashed curve. Again the energy difference between these states is approximately $2\pi/L$.

States with two flipped spins have a much larger energy; the state with lowest energy and $M=3$ lies about $8\pi/L$ above the ground state. It is also important to point out that so far we only considered elementary excitations. Excitations can, however, also be combined; i.e., charge, ''string''-type, and spin-flip excitations can be superimposed by changing the quantum numbers accordingly. These more complex excitations typically have higher energies. In the thermodynamic limit this superposition is particularly simple and reduced to a *linear* superposition; i.e., the excitation energies become additive.

IV. CONCLUSIONS

We studied the low-energy excitation spectrum of a spherical nanosized metallic particle with an Anderson impurity ($U\rightarrow\infty$) at its center. Due to the finite dimension of the particle, the energy spectrum is discrete. Only *s* waves interact with the impurity (assuming a contact hybridization), such that only a reduced number of host states need to be considered. At low and intermediate temperatures the properties depend crucially only on the average spacing of the host states close to the Fermi level. We chose a linear rela-

tion between energy and wave numbers for the *s* states, which has several advantages: namely, (i) the model can be mapped onto the integrable variant of the Anderson problem, previously solved via Bethe's *Ansatz*,[2,11,12] (ii) it corresponds to a constant density of states for *s* states in the thermodynamic limit (an assumption usual in treatments of the Kondo problem), and (iii) the scaling of the energy levels with the size of the system L in the thermodynamic limit leads to the conformal towers for the excitations.

The usual formulation of the Anderson impurity model (in terms of electrons and the f^0 and f^1 configurations) yields Bethe *Ansatz* equations with complex-conjugated charge rapidities for the ground state. Unfortunately, the equations determining the real and imaginary parts are nonlinear and have, in general, many solutions. It is difficult to determine the physical ground state. This is the consequence of an ''effective'' attraction between the charges that leads to spin-paired singlet states represented by complex-conjugated pairs of rapidities. The ambiguities in the solutions only occurs in a finite system, but not in the thermodynamic limit. A similar situation appears for the supersymmetric *t-J* model in a finite box if the Bethe *Ansatz* is formulated within the Lai representation.[15,16] On the other hand, if instead the Bethe *Ansatz* is formulated within the Sutherland representation[17] (in terms of a graded algebra), the rapidities for the ground state are all real.

To bypass these ambiguities, in Sec. III we reformulate the model and the Bethe *Ansatz* for the Anderson impurity in terms of the f^1 and f^2 configurations (these are the hole configurations corresponding to the electron f^0 and f^1 configurations). This is the analog to using the Sutherland representation rather than the Lai formulation for the supersymmetric *t-J* model. Now all charge and spin rapidities are real in the ground state and the situation is closely related to the previous finite-size studies of Bethe states for the Heisenberg chain[14] and the Kondo problem.[10]

The states are characterized by integer (half-integer) quantum numbers for the charge and spin rapidities. The ground state corresponds to compact sets of consecutive integers or half-integers (without leaving ''holes''). The energy of the system increases monotonically and continuously with increasing *f*-level energy. Charge excitations are obtained by introducing holes into the set of charge quantum numbers. Similarly, low-energy spin-singlet or non-spin-flip excitations are obtained by introducing holes into the set of spin quantum numbers and through strings of complex spin rapidities. On the other hand, spin-flip excitations are obtained by reducing the number of flipped spins M.

We calculated the ground-state energy and the lowest-energy charge and spin excitations as a function of ϵ_f. These excitation energies constitute the dominating activation gaps in the low-T specific heat and susceptibility due to the finite size of the system. The charge and spin gaps are comparable in magnitude and only weakly dependent on ϵ_f. (This contrasts with the situation for the Kondo exchange model where the excitation gap without spin flip is smaller than the spin-flip gap). The gaps decrease with increasing particle size and in the thermodynamic limit the finite-size corrections to the energy are given by the conformal towers. In this limit the gaps are infinitesimally small and the system is a Fermi liquid; i.e., the susceptibility is finite and the specific heat is proportional to T.

Finally, an Anderson impurity embedded in a small particle is related to a single-electron quantum dot embedded or as a side branch coupled to a short quantum wire.[6,7] In this case the valence (or ϵ_f) can be changed with a bias voltage and the magnetization of the dot with a magnetic tip. As a consequence of the gaps in the spin excitation spectrum the magnetization at $T=0$ shows plateaus as a function of field. The magnetization is then stable to fluctuations in the magnetic field. At low T the steps in the magnetization are rounded off, but the step structure remains, such that the system could be used as a magnetic storage device.

ACKNOWLEDGMENTS

Support by the National Science Foundation under Grant No. DMR01-05431 and the Department of Energy under Grant No. DE-FG02-98ER45797 is acknowledged. The author would like to thank A.A. Zvyagin for helpful comments.

[1] A.M. Tsvelick and P.B. Wiegmann, Appl. Acoust. **32**, 453 (1983).
[2] P. Schlottmann, Phys. Rep. **181**, 1 (1989).
[3] W.A. de Heer, Rev. Mod. Phys. **65**, 611 (1993).
[4] M. Brack, Rev. Mod. Phys. **65**, 677 (1993).
[5] W.B. Thimm, J. Kroha, and J. von Delft, Phys. Rev. Lett. **82**, 2143 (1999).
[6] M. Buttiker and C.A. Stafford, Phys. Rev. Lett. **76**, 495 (1996).
[7] P. Schlottmann and A.A. Zvyagin, Phys. Lett. A **231**, 109 (1997).
[8] N. Andrei, Phys. Rev. Lett. **45**, 379 (1980).
[9] P.B. Wiegmann, Pis'ma Zh. Éksp. Teor. Fiz. **31**, 392 (1980) [JETP Lett. **31**, 364 (1980)].
[10] P. Schlottmann, Phys. Rev. B **65**, 024420 (2002).
[11] P. Schlottmann, Z. Phys. B: Condens. Matter **49**, 109 (1982).
[12] P. Schlottmann, Z. Phys. B: Condens. Matter **59**, 391 (1985).
[13] If the model is formulated on a lattice, then $L>N$, but in the continuum there is no restriction for L.
[14] M. Karbach and G. Müller, Comput. Phys. **11**, 36 (1997); M. Karbach, K. Hu, and G. Müller, *ibid.* **12**, 565 (1998).
[15] C.K. Lai, J. Math. Phys. **15**, 1675 (1974).
[16] P. Schlottmann, Phys. Rev. B **36**, 5177 (1987).
[17] B. Sutherland, Phys. Rev. B **12**, 3795 (1975).